Crustal Deformation Associated with the Seismic Cycle in the Central Andes from InSAR and GNSS Geodetic Time Series

Bertrand Lovery[1], Anne Socquet[1], Mohamed Chlieh[1], Marie-Pierre Doin[1], Mathilde Radiguet[1], Juan Carlos Villegas-Lanza[2], Juliette Cresseaux[1], Edmundo Norabuena[2], Philippe Durand[3]

[1]ISTerre, Université Grenoble Alpes, CNRS, IRD, Grenoble, France
[2]Instituto Geofísico del Perú (IGP), Lima, Peru
[3]CNES, Toulouse, France

corresponding author: bertrand.lovery@univ-grenoble-alpes.fr

Interseismic Coupling and Megathrust Earthquake Potential on the South Peru subduction

The Central Andes subduction has been the theatre of **several large earthquakes** since the beginning of the 21th century:
→ 2001 Mw8.4 Arequipa, 2007 Mw8.0 Pisco, 2014 Mw8.1 Iquique earthquakes

In Lovery et al. (2024) we analyzed **73 GNSS points covering the last decade** to extract the interseismic velocity field. This field has been inverted to model the interseismic coupling distribution at the scale of South Peru in an elastic half-space. Then, by performing a moment budget analysis (Avouac, 2015), we are able to estimate the **potential maximum magnitude earthquake** in the area, with the associated recurrence time.

The **interseismic coupling** (or locking) quantifies how locked the plate interface is. **Interseismic coupling** is defined between **0** (plates are **slipping** without any friction) and **1** (plates are fully **locked**)

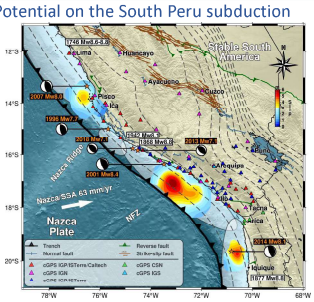

Seismotectonic background of the Central Andes subduction zone. The slip models for the M_w8.0 2007 Pisco (Chlieh et al., 2011), M_w8.4 2001 Arequipa (Lovery et al., 2024), and M_w8.1 2014 Iquique (Lovery et al., 2024) earthquakes are displayed in colors along the subduction interface. Triangles show the location of GNSS stations.

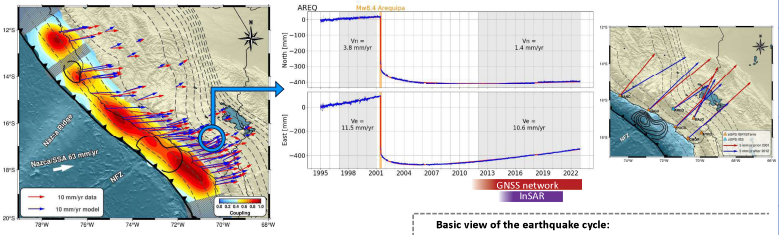

→ During the observation period in this study (2012-2023 for most stations), the observed interseismic velocity at AREQ is reduced by about 15% relative to its value before 2001

→ **What is the impact of postseismic relaxation on interseismic loading?**

→ **Can we extend the spatial coverage of measurements with InSAR?**

Basic view of the earthquake cycle:

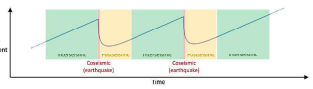

→ **Postseismic** can be caused by:
- aseismic slip on the fault (afterslip) → medium-term
- viscoelastic relaxation in the asthenosphere → long-term
- poroelastic rebound → short-term

Evidence for a Peruvian Sliver?

We inverted the interseismic velocities corrected from the rigid block motion defined by Villegas et al. (2016), the so-called **Peruvian Sliver (PS)**. The results tend to accredit the Peruvian Sliver hypothesis, with a lowered misfit and a more sensible locking depth.

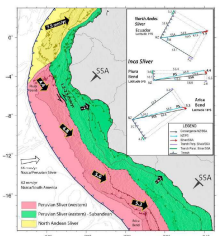

Figure from Villegas et al. (2016) defining the so-called Peruvian Sliver. The rigid block motion has been defined from the residuals of the inversion in the Stable South America frame.

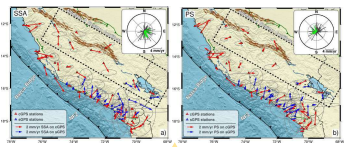

Residuals from our inversions using GNSS data in the SSA frame (a) and in the PS frame (b). Residuals at inland stations, within the black dashed rectangle, are highlighted in green on the roses.

Moment budget analysis and earthquake potential:

We performed a **moment budget** at the scale of the **South Peru segment**, from the Nazca Ridge to the Arica bend. This methodology, described in Avouac (2015), balance the seismicity rate with the moment deficit rate on the megathrust interface to estimate the earthquake potential in the area. 864 combinations of these parameters have been computed, following the logic tree on the right. The b-value of instrumental catalogues as well as the amount of aseismic slip in the transient slips (alpha) are the two parameters that show the largest variability in the determination of the Mmax.

→ **Overall, we found a median value of Mw=8.55, a 15th percentile at Mw=8.15, and a 85th percentile at Mw=9.0**. Considering the largest earthquake recorded on the South Peru segment was the 2001 Mw=8.4 Arequipa earthquake, we can state that the earthquake potential on this segment is at least Mw=8.4. The recurrence time for a Mw=8.4 would be ~100 years, while it would be ~1,000 years for a Mw=9.0.

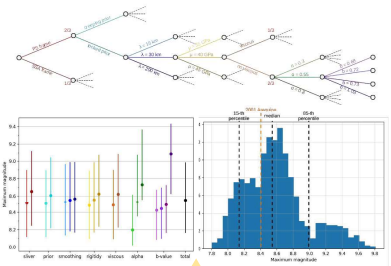

Top: Logic tree used for exploration of uncertainties.
Bottom left: Earthquake potential in function of the parameters. The dots represent the median Mw value, while the vertical bars represent the variability between the 15th and 85th percentiles on the 864 models considered.
Bottom right: Distribution of the earthquake potential, accounting for all the discussed factors of uncertainty. Median, 15th and 85th percentiles are depicted by dashed lines.

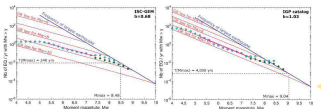

Estimation of maximum expected magnitude with $\alpha = 0.7$ and $\mu = 40$ GPa, in the PS frame and with a smoothing $\lambda = 30$ km, for the ISC-GEM catalog (left) and the IGP catalog (right). Instrumental earthquakes from the catalogs are depicted by cyan dots, historical earthquakes from Villegas et al. (2016) by green dots.

Conclusions

→ 2001 M_w8.4 Arequipa earthquake postseismic relaxation is still ongoing

→ Accounting for the viscoelastic relaxation following the 2001 Arequipa earthquake increases the moment deficit by 6%, but remains within uncertainties with M_{max} ranging from M_w=8.4 to M_w=9.0 (Lovery et al., 2024)

→ The Nazca Ridge can be assumed as a strong barrier, however the Nazca Fracture Zone can only be seen as a weak barrier

Next challenges

→ Inversion of interseismic velocities with viscoelastic Green functions

→ We expect a viscoelastic model to produce a broader displacement, with horizontal displacements extending further inland. Uplift and subsidence amplitudes are also expected to increase with a viscoelastic rheology.
→ Viscoelastic models should also predict higher magnitudes of deformation in the late stage of the interseismic period, especially in the near-field and in the far-field.
→ Finally, a shallower optimal locking depth for visco-elastic models is expected.

→ Combine GNSS and InSAR in a joint inversion of interseismic at the scale of the central Andes

→ Discriminate slip on the slab interface from internal deformation, benchmarking the solid sliver motion hypothesis

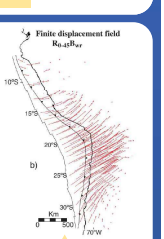

Figure from Arriagada et al. (2008), showing Paleogene to present displacement vectors from paleomagnetism analysis.

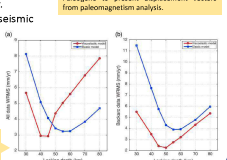

Figure from Li et al. (2015) . Comparison between elastic and viscoelastic models, for horizontal displacement (a) and vertical displacement (b).

Postseismic viscoelastic FEM model

In order to assess the local rheology, we carried out a case study on the **2001 Mw8.4 Arequipa earthquake** using a **postseismic viscoelastic FEM model** of the subduction. Our model is constrained by the timeseries of the AREQ continuous GNSS station, operating since 1993 in Arequipa.

→ 3-D FEM model solved using PyLith, meshing performed with Coreform CUBIT
→ Slab contours from Slab2 (Hayes, 2018), Bathymetry & topography from SRTM15+

→ "Cold-nose" up to 85-km depth
→ Bi-viscous **Burger** rheology in the asthenosphere

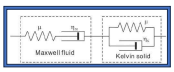

Burger body

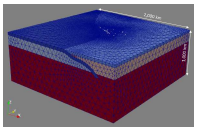

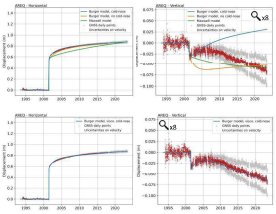

→ The blue model fits the horizontal but not the long-term vertical

→ Fitting the vertical requires a low-viscosity zone in the cold-nose

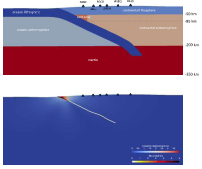

→ We compute the velocities associated with the viscoelastic relaxation during the observation period of the GNSS network used for interseismic coupling modelling (~2012-2024), at each GNSS sites

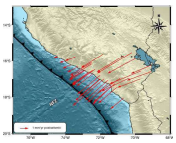

Body	Rheology	Depth (km)	Shear modulus (GPa)	Maxwell viscosity (Pa.s)	Kelvin viscosity (Pa.s)
Lithosphere	Elastic	0 - 40	59	-	-
Cold nose	Maxwell	40 - 85	70	1.10^{20}	-
Upper asthenosphere	Burger	40 - 200	70	1.10^{19}	5.10^{18}
Lower asthenosphere	Maxwell	200 – 1,000	105 - 294	5.10^{20}	-

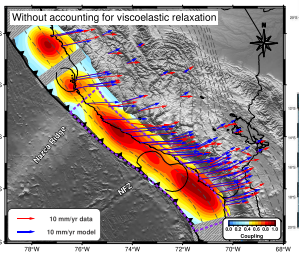

Viscoelastic correction

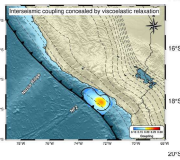

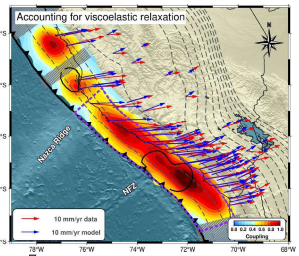

Higher coupling in the Southern segment, no more creeping where the NFZ is subducting

Moment deficit on the Nazca-Arica segment:

$\frac{dM_0}{dt} = 2.24 \times 10^{20}$ Nm/yr, without accounting for relaxation
→ M_{max} ~ 8.70

$\frac{dM_0}{dt} = 2.37 \times 10^{20}$ Nm/yr, accounting for relaxation (+6%)
→ M_{max} ~ 8.73

Large-scale InSAR coverage - FLATSIM Andes project

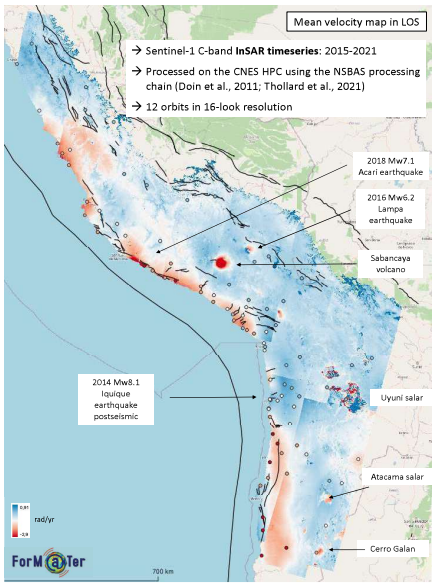

→ Sentinel-1 C-band **InSAR timeseries**: 2015-2021
→ Processed on the CNES HPC using the NSBAS processing chain (Doin et al., 2011; Thollard et al., 2021)
→ 12 orbits in 16-look resolution

Modelling ocean tide loading (OTL), solid Earth tides (SET), and total electronic content (TEC):

→ SET show strong correlation in range

→ TEC shows good correlation on ascending tracks (acquisition time in the evening)

→ OTL shows moderate correlation. This correlation is improved by removing SET and TEC from the FLATSIM ramps, the OTL signal being significantly smaller

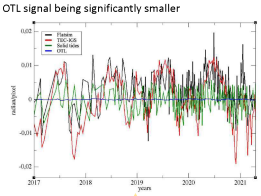

Ramps in range removed during the FLATSIM time series inversion (black) for the A076N track, with modelled IGS TEC ramps (red), SET ramps (green), and OTL ramps (blue)

Ramps in range removed during the FLATSIM time series inversion (black) for the A076N track, with modelled IGS TEC ramps (red), SET ramps (green), and OTL ramps (blue)

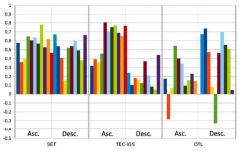

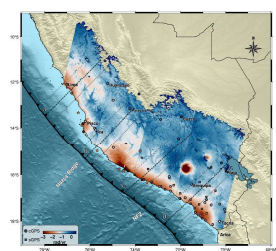

Viscoelastic correction

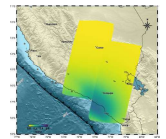

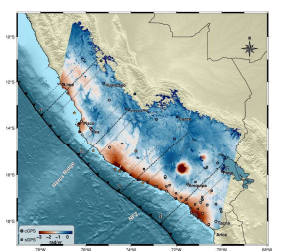

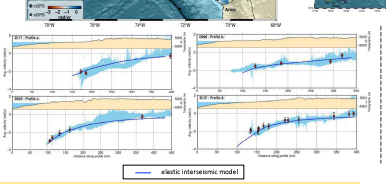

Mean velocity map (2015-2021) in LOS on descending tracks. Corrected from the 2018 Mw7.1 Acari (model from J. C. Villegas-Lanza) and 2014 Mw8.1 Iquique earthquakes (Lovery et al., 2024)

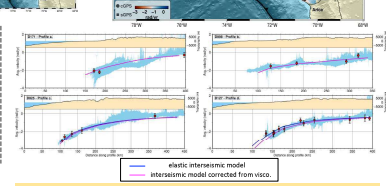

Mean velocity map (2015-2021) in LOS on descending tracks. Corrected from the 2018 Mw7.1 Acari (model from J. C. Villegas-Lanza) and 2014 Mw8.1 Iquique earthquakes (Lovery et al., 2024) + viscoelastic

References:

Arriagada, C., Roperch, P., Mpodozis, C., & Cobbold, P. R. (2008). Paleogene building of the Bolivian Orocline: Tectonic restoration of the central Andes in 2-D map view. *Tectonics*, *27*(6). https://doi.org/10.1029/2008TC002269

Avouac, J.-P. (2015). From Geodetic Imaging of Seismic and Aseismic Fault Slip to Dynamic Modeling of the Seismic Cycle. *Annual Review of Earth and Planetary Sciences*, *43*(1), 233–271. https://doi.org/10.1146/annurev-earth-060614-105302

Doin, M.-P., Guillaso, S., Jolivet, R., Lasserre, C., Lodge, F., Ducret, G., & Grandin, R. (2011). Presentation of the small baseline NSBAS processing chain on a case example: The Etna deformation monitoring from 2003 to 2010 using Envisat data. In *Proceedings of the Fringe symposium* (pp. 3430–3437). ESA SP-697, Frascati, Italy.

Lovery, B., Chlieh, M., Norabuena, E., Villegas-Lanza, J. C., Radiguet, M., Cotte, N., et al. (2024). Heterogeneous locking and earthquake potential on the South Peru megathrust from dense GNSS network. *Journal of Geophysical Research: Solid Earth*, *129*, e2023JB027114. https://doi.org/10.1029/2023JB027114

Luo, H., & Wang, K. (2021). Postseismic geodetic signature of cold forearc mantle in subduction zones. *Nature Geoscience*, *14*(2), 104–109. https://doi.org/10.1038/s41561-020-00679-5

Marill, L., Marsan, D., Socquet, A., Radiguet, M., Cotte, N., & Rousset, B. (2021). Fourteen-Year Acceleration Along the Japan Trench. *Journal of Geophysical Research: Solid Earth*, *126*(11), e2020JB021226. https://doi.org/10.1029/2020JB021226

Radiguet, M., Cotton, F., Vergnolle, M., Campillo, M., Valette, B., Kostoglodov, V., & Cotte, N. (2011). Spatial and temporal evolution of a long term slow slip event: the 2006 Guerrero Slow Slip Event. *Geophysical Journal International*, *184*(2), 816–828. https://doi.org/10.1111/j.1365-246X.2010.04866.x

Thollard, F., Clesse, D., Doin, M.-P., Donadieu, J., Durand, P., Grandin, R., et al. (2021). FLATSIM: The ForM@Ter Large-Scale Multi-Temporal Sentinel-1 InterferoMetry Service. *Remote Sensing*, *13*(18), 3734. https://doi.org/10.3390/rs13183734

Villegas-Lanza, J. C., Chlieh, M., Cavalié, O., Tavera, H., Baby, P., Chire-Chira, J., & Nocquet, J.-M. (2016). Active tectonics of Peru: Heterogeneous interseismic coupling along the Nazca megathrust, rigid motion of the Peruvian Sliver, and Subandean shortening accommodation. *Journal of Geophysical Research: Solid Earth*, *121*(10), 7371–7394. https://doi.org/10.1002/2016JB013080

Wang, K., Hu, Y., & He, J. (2012). Deformation cycles of subduction earthquakes in a viscoelastic Earth. *Nature*, *484*(7394), 327–332. https://doi.org/10.1038/nature11032

Acknowledgements:

Bertrand Lovery's PhD is funded by the French national space agency CNES and the DEEPtrigger ERC project (PI: Anne Socquet).